Atom recoil in collectively interacting dipoles using quantized vibrational states

Deepak A. Suresh [1] and F. Robicheaux [1,2,*]

[1]*Department of Physics and Astronomy, Purdue University, West Lafayette, Indiana 47907, USA*

[2]*Purdue Quantum Science and Engineering Institute, Purdue University, West Lafayette, Indiana 47907, USA*

(Received 18 November 2021; accepted 15 February 2022; published 4 March 2022)

The recoil of atoms in dense ensembles during light-matter interactions is studied using quantized vibrational states for the atomic motion. The recoil resulting from the forces due to the near-field collective dipole interactions and far-field laser and decay interactions are explored. The contributions to the recoil and the dependence on the trap frequency of the different terms of the Hamiltonian and Lindbladian are studied. These calculations are compared with previous results using the impulse model in the slow-oscillation approximation. Calculations in highly subradiant systems show enhanced recoil indicating that recoil effects cannot be ignored in such cases.

DOI: 10.1103/PhysRevA.105.033706

I. INTRODUCTION

The study of collective dipole-dipole interactions has progressed significantly since Dicke pioneered the idea in 1954 [1–12]. There have been many recent innovations using collective interactions in coherent quantum control and quantum information [13–20]. As an example, atom arrays which are densely packed have been shown to have high reflectivity [21–23]. But as the atoms get closer and denser, the forces due to the collective interactions become larger, causing the internal states to become entangled with the vibrational motion of the atom. This causes unwanted decoherences to arise in the system. There is a need to better understand the forces involved with the collective dipole interactions and the role that recoil plays in the coherence of the system.

These questions motivated us in Refs. [24,25], in which we studied the recoil in the atoms in light-matter interactions in densely packed ensembles and atom arrays. More specifically, in Ref. [25], we described a model to calculate the recoil in atoms in which the photon recoil is considered an impulsive force. This model will be referred to as the impulse model in this paper. It was constructed under slow oscillation, or, equivalently, sudden approximation, where the timescales of the atomic oscillations are much longer than the timescales of the internal-state dynamics. This implies that the trap frequencies should be much smaller than the decay rate of the system.

Typically, the trap frequencies used are 10 to 100 kHz, while the decay rates of electronic excitations are often around tens of megahertz. While these trap-frequency ranges would normally be within the sudden approximation, problems arise when the system becomes subradiant and the collective decay rates approach the trap frequencies. The results from the impulse model also indicated that the recoil is typically proportional to the lifetime of the excitation in certain cases, leading to enormous recoils in highly subradiant systems. While the sudden approximation gives an intuitive understanding of how energy is added to the center-of-mass motion and how decoherence arises, the assumptions in the approximation are dubious for some of the more interesting atomic arrangements. The goal of this paper is to clarify such ambiguous results and to extend the analysis beyond the approximations used in Ref. [25].

The quantum harmonic-oscillator model described in this paper calculates the recoil in collectively interacting systems but removes the assumptions in the sudden approximation. N atoms are assumed to be trapped in harmonic potentials having quantized vibrational energy states. Using the density-matrix formalism, we time evolve the combined vibrational and internal-state density matrix to calculate the momentum and energy deposited in the system at a later time. This model does not have the limitation of the sudden approximation and can be used to simulate a wide range of trap frequencies and thus can serve as an important test of the sudden approximation. It will also provide insight into how the different terms of the Hamiltonian and the Lindblad operator contribute to the recoil of the atoms. We focus on the transfer of energy in the system rather than the vibrational population as the population in the excited states trivially decreases as the frequency increases for the same energy transfer.

To simplify the calculations, we will work in the low-intensity limit where there is only a single excitation in the system; that is, only one atom can be electronically excited at a time. This will reduce the number of internal states from 2^N to $(N+1)$. We also investigate only cases where the spread of the atomic wave function is smaller than the distances of atom separation to reduce the overlap of wave functions. This is expected in reasonable experimental arrangements because otherwise, the atom grid is not well defined.

This paper proceeds as follows. Section II discusses the model and equations used. Section III A discusses the decay and laser interaction for a single atom to illustrate the role of recoil, and Sec. III B extends the analysis to N atoms. We

*robichf@purdue.edu

discuss approximations to simulate a large number of atoms in Sec. III C to calculate the recoil in arrays of atoms and subradiant cavities. Section IV presents the conclusions and summarizes the results and future outlook.

II. METHODS

We shall consider N atoms, each trapped in a quantum harmonic potential with each atom having two internal electronic states. The center of each trap will form a spatial arrangement required by the experiment, for example, a square array. Since the atoms are in a harmonic trap potential, they will each have an infinite Hilbert space of vibrational levels. We can limit the number of vibrationally excited states for each atom to states $n < N_{\text{vib}}$ for calculation purposes. When the spread of the atomic wave function is small, the effects on the harmonic-oscillator wave functions are separable across the different directions. Hence, we can run the calculations by choosing one oscillation direction at a time. The N atoms together will have a combined vibrational Hilbert space of $V = (N_{\text{vib}})^N$ states. Since we are working in the low-intensity limit and only one atom can be electronically excited at any time, the total number of internal states is $N + 1$. Hence, the total number of states is $(N + 1)(N_{\text{vib}})^N$.

The internal states will be represented by $|j\rangle$, the collective vibrational states will be represented by $|m\rangle$, and the total state will be denoted by $|j, m\rangle$. The internal-state index goes from zero to N, where $j = 0$ represents the electronic ground state (alternatively, $|g\rangle$) with no atom excited and $j = 1$ to N represent only the jth atom being excited. The collective vibration state $|m\rangle$ is the tensor product of all possible vibrational states, i.e., $|m\rangle = |n_1\rangle \otimes |n_2\rangle \otimes \otimes |n_N\rangle$, where $|n_i\rangle$ is the vibrational state of the ith atom. The index m goes from $m = 0$ to $(N_{\text{vib}})^N - 1$.

Hence, the density matrix will be represented by

$$\rho = \sum_{j,j'} \sum_{m,m'} \rho_{j,j'}^{m,m'} |j, m\rangle\langle j', m'|. \tag{1}$$

The density matrix evolves according to the equation given by

$$\frac{d\hat{\rho}}{dt} = -\frac{i}{\hbar}[\hat{H}, \hat{\rho}] + \mathcal{L}(\hat{\rho}), \tag{2}$$

where $\hat{\rho}$ is the density matrix of the system, $\hat{H}$ is the effective Hamiltonian, and $\mathcal{L}(\hat{\rho})$ is the Lindblad superoperator. The effective Hamiltonian consists of three parts: (1) the trap potential of the atoms, which is a quantum harmonic-oscillator Hamiltonian, (2) the laser Hamiltonian, and the (3) dipole-dipole resonant interaction.

The Hamiltonian of the trap potential is given by

$$H_t = \sum_j \hbar\omega_t \left(a_j^\dagger a_j + \frac{1}{2}\right), \tag{3}$$

where ω_t is the trap frequency of the harmonic oscillator and $a_j^\dagger$ and a_j are the harmonic-oscillator ladder operators for the jth atom in the chosen direction. The mean position of the wave function or the fixed point positions of the atoms will be given by $\mathbf{R}_j$, and the spread of the atom or the position of the atom with respect to the mean will be given by $\mathbf{r}_j$. The position operator along the chosen direction is given by $s_j = \sqrt{\frac{\hbar}{2M\omega_t}}(a_j + a_j^\dagger)$. We define the quantity $\kappa = k\sqrt{\frac{\hbar}{2M\omega_t}}$, where the length scale for the atoms' motion and the spread of the atomic wave function is described by κ/k. Here, k is the wave number of the resonant light, and M is the mass of a single atom.

When the laser interacts with the atoms, it imparts a momentum of $\hbar k$ which will manifest in the Hamiltonian through the position operators s_j. The Hamiltonian due to the laser is

$$\hat{H}_L = \hbar \sum_j \left[-\delta\hat{\sigma}_j^+\hat{\sigma}_j^- + \left(\frac{\Omega}{2}\hat{\sigma}_j^+ e^{i\mathbf{k}_0\cdot(\mathbf{R}_j+\hat{\mathbf{r}}_j)} + \text{H.c.}\right)\right]. \tag{4}$$

where Ω is the Rabi frequency, δ is the detuning, and $\mathbf{k}_0 = k\hat{\mathbf{z}}$ is the initial wave vector of the incoming photons. $\hat{\sigma}_j^+$ and $\hat{\sigma}_j^-$ are the raising and lowering operators of the electronic excitation of the jth atom. If the laser is propagating in the chosen direction of vibrational oscillation, the term $\mathbf{k}_0 \cdot \mathbf{r}_j$ can be replaced by $\kappa(\hat{a}_j + \hat{a}_j^\dagger)$. Otherwise, the $\mathbf{k}_0 \cdot \mathbf{r}_j$ term will be dropped, and the laser will not cause any vibrational transitions.

In the following equations, the primed and unprimed coordinates are used to signify right and left multiplication of the density operator, respectively. To signify differences, we will use the following convention:

$$\mathbf{r}_{ij} \equiv \mathbf{r}_i - \mathbf{r}_j, \quad \mathbf{r}'_{ij} \equiv \mathbf{r}_i - \mathbf{r}'_j, \quad \mathbf{r}''_{ij} \equiv \mathbf{r}'_i - \mathbf{r}'_j. \tag{5}$$

The resonant dipole-dipole interactions are given by the imaginary part of the Lindblad term and are given by

$$\hat{H}_{dd} = \hbar \sum_{i\neq j} \text{Im}\{g(\mathbf{R}_{ij} + \mathbf{r}_{ij})\}\hat{\sigma}_i^+\hat{\sigma}_j^-. \tag{6}$$

The real part of the Lindblad term describes the dynamics of the decay and is given by

$$\begin{aligned}\mathcal{L}(\hat{\rho}) = \sum_{i,j} [&2\text{Re}\{g(\mathbf{R}_{ij} + \mathbf{r}'_{ij})\}\hat{\sigma}_i^-\hat{\rho}\hat{\sigma}_j^+ \\ &- \text{Re}\{g(\mathbf{R}_{ij} + \mathbf{r}_{ij})\}\hat{\sigma}_i^+\hat{\sigma}_j^-\hat{\rho} \\ &- \hat{\rho}\hat{\sigma}_i^+\hat{\sigma}_j^-\text{Re}\{g^*(\mathbf{R}_{ij} + \mathbf{r}''_{ij})\}],\end{aligned} \tag{7}$$

where the Green's function $g(\mathbf{R})$ is given by

$$g(\mathbf{R}) = \frac{\Gamma}{2}\left[h_0^{(1)}(kR) + \frac{3(\hat{R}\cdot\hat{q})(\hat{R}\cdot\hat{q}^*) - 1}{2}h_2^{(1)}(kR)\right], \tag{8}$$

where $\hat{q}$ is the dipole orientation, $R = |\mathbf{R}|$ is the norm of $\mathbf{R}$, $\hat{R} = \mathbf{R}/R$ is the unit vector along $\mathbf{R}$, Γ is the decay rate of a single atom, and $h_l^{(1)}(x)$ is the outgoing spherical Hankel function of angular momentum l; $h_0^{(1)}(x) = e^{ix}/[ix]$, and $h_2^{(1)}(x) = (-3i/x^3 - 3/x^2 + i/x)e^{ix}$.

When we calculate the Green's function, we take a Taylor expansion up to second order which is valid under the condition that the spread of the wave function (κ/k) is much less than the separation of atoms:

$$\begin{aligned}g(\mathbf{R}_{ij} + \epsilon) = g(\mathbf{R}_{ij}) &+ \left(\frac{g'(\mathbf{R}_{ij})}{k}\right)k\epsilon \\ &+ \left(\frac{g''(\mathbf{R}_{ij})}{k^2}\right)\frac{k^2\epsilon^2}{2} + \cdots,\end{aligned} \tag{9}$$

where the derivatives are taken in the chosen oscillation direction. Since the Hankel functions in $g(R)$ are functions of kR, the k's in the denominators make the expansion term $k\epsilon$ more explicit. $\epsilon = s_i - s_j$ is expanded into the corresponding vibrational ladder operators. The zeroth-order term does not depend on the spread of the atoms and does not cause any transitions in the vibrational state. The first- and second-order terms depend on the spread of the wave function and will induce single-level and two-level transitions in the vibrational states, respectively.

Since the Green's function depends on both $\mathbf{r}_j$ and $\mathbf{r}'_j$, which correspond to the left and right operations on the density matrix, we have s_j and s'_j, respectively. While the last two terms of the Lindblad expression have only left or right multiplication, the first term behaves differently. Upon expanding the Harmonic vibrational wave functions, we see that the first term acts on the combined density matrix as

$$\begin{aligned}
&\mathrm{Re}\{g(R_{ij}+r'_{ij})\}\hat{\sigma}_i^-\hat{\rho}\hat{\sigma}_j^+ \\
&\quad = \mathrm{Re}\{g(R_{ij})\}\hat{\sigma}_i^-\hat{\rho}\hat{\sigma}_j^+ \\
&\qquad + \mathrm{Re}\left\{\frac{g'(R_{ij})}{k}\right\}k(s_i\hat{\sigma}_i^-\hat{\rho}\hat{\sigma}_j^+ - \hat{\sigma}_i^-\hat{\rho}\hat{\sigma}_j^+ s'_j) \\
&\qquad + \mathrm{Re}\left\{\frac{g''(R_{ij})}{k^2}\right\}\frac{k^2}{2}\big(s_i^2\hat{\sigma}_i^-\hat{\rho}\hat{\sigma}_j^+ + \hat{\sigma}_i^-\hat{\rho}\hat{\sigma}_j^+ s_j'^2 \\
&\qquad - 2s_i\hat{\sigma}_i^-\hat{\rho}\hat{\sigma}_j^+ s'_j\big),
\end{aligned} \tag{10}$$

where the ks_i's will be replaced by $\kappa(a_i + a_i^\dagger)$ notation when solving the equations. The expectation values of the momentum and energy in the vibrational state of atom j can then be calculated from the density matrix,

$$p_j = \frac{i}{2\kappa}\mathrm{Tr}[(a_j^\dagger - a_j)\rho]\hbar k, \tag{11}$$

$$E_j = \frac{1}{2\kappa^2}\mathrm{Tr}[(2a_j^\dagger a_j + 1)\rho]E_r, \tag{12}$$

where $\hbar k$ and $E_r = \hbar^2k^2/(2M)$ are the recoil momentum and energy deposited when one photon is absorbed or emitted by an atom. Since the expression for the energy is divided by κ^2, only the terms of the order of κ^2 in the diagonal of the density matrix will primarily contribute to a change in energy. The contribution from the κ^4 terms and beyond will be negligible for small wave-function spreads. The energy difference in the vibrational levels will be given by $1/\kappa^2$. That is, if $\kappa = 0.01$, the energy difference of consecutive vibrational levels will be 10^4E_r.

III. RESULTS

The impulse model used in Ref. [25] calculates the kinetic energy and momentum kick imparted in a collective dipole interaction system interacting with a laser. Since the quantum oscillator model discussed in this paper has a fundamental difference in the way the kinetic energy is imparted to the system, the two models can be compared and tested for validity. To account for the spread of the wave function, the impulse model can be spatially integrated over the wave-function probability density using Gaussian quadrature integration for a small number of atoms. At low frequencies, the sudden approximation is valid, and the models agree. The results match exactly at low wave-function spreads and with a small difference for higher spreads. This difference can be shown to be due to stopping at the second order when expanding $g(R)$ in the Taylor series; that is, the error is mainly in the harmonic-oscillator model for low trap frequencies.

The quantum oscillator model does not have any restrictions with respect to the trap frequency, and hence, we can investigate the validity of the sudden approximation, beyond the low-frequency regime. We can also study the separate contributions from the different terms of the Hamiltonian and the Lindblad equations. We are more interested in the cases with higher trap frequencies where the vibrational energy spacing is much larger than E_r. Hence, we do not need to include many vibrational levels. This also implies that the spread of the wave function will be small and we can limit the Taylor-series expansion, Eq. (9), to second-order terms.

A. Single-atom decay

To begin, we analyze the simple decay process of a single atom trapped in a harmonic potential. The atom is initially excited, and no laser interaction is present. The effective Hamiltonian becomes

$$H_t = \hbar\omega_t(a_1^\dagger a_1 + 1/2). \tag{13}$$

Since H_t is purely diagonal with respect to the vibrational states, its contribution to the change in the density matrix,

$$\dot{\rho} = \frac{-i}{\hbar}[H_t, \rho], \tag{14}$$

has zero diagonal elements and interacts with only the off-diagonal coherence terms of the density matrix. The Lindblad term for a single atom is

$$\begin{aligned}
\mathcal{L}^{(1)}(\rho) = {}& 2\mathrm{Re}\{g(r'_{11})\}\sigma_1^-\rho\sigma_1^+ \\
& - \mathrm{Re}\{g(r_{11})\}\sigma_1^-\sigma_1^+\rho - \rho\sigma_1^-\sigma_1^+\mathrm{Re}\{g(r''_{11})\}.
\end{aligned} \tag{15}$$

Since $r_{11} = r''_{11} = 0, \mathrm{Re}\{g(r_{11})\} = \mathrm{Re}\{g(r''_{11})\} = \Gamma/2$. The last two terms do not contribute to change in the vibrational states. Expanding the first term using $r'_{11} = 0 + s_1 - s'_1$ up to second order gives

$$\mathrm{Re}\{g(r'_{11})\} = g(0) + \frac{g''(0)}{2}\kappa^2(s_1 - s'_1)^2 \tag{16}$$

κ is defined below Eq. (3), since the first derivative $g'(0) = 0$. The next nonzero leading-order term will be fourth order since the third derivative is again zero, but they will be of the order of κ^4 and will not cause significant contributions when calculating the energy. If we assume the atom is initially excited and in the vibrational ground state, the first term in Eq. (15) becomes

$$\begin{aligned}
\mathcal{L}_1(\rho) = {}& |g\rangle\langle g|\rho_{1,1}^{0,0}\{[\Gamma + 2\kappa^2 g''(0)]\,|0\rangle\langle 0| \\
& - 2\kappa^2 g''(0)\;\;|1\rangle\langle 1| + \kappa^2 g''(0)\sqrt{2}(|2\rangle\langle 0| + |0\rangle\langle 2|)\}.
\end{aligned} \tag{17}$$

We can analytically solve the above equation to obtain the change in the vibrational energy at infinite time when the decay is complete. The change in vibrational energy is given

by

$$\Delta E = -2\frac{g''(0)}{\Gamma}E_r. \tag{18}$$

This result remains valid when the initial density matrix is any incoherent combination of vibrational states. For an atom initially excited and polarized in the $e_+ = -(\hat{\mathbf{x}} + i\hat{\mathbf{y}})/\sqrt{2}$ direction, $\Delta E_z = 0.4E_r$, and $\Delta E_x = \Delta E_y = 0.3E_r$. The energy deposited due to the recoil from the emission of a single photon is independent of the frequency of the harmonic oscillator. This result is correct even if we go beyond the second-order approximation in Eq. (16).

1. Laser interaction

When the atom absorbs a single photon from the laser, there is a momentum of $\hbar k$ added to the atom. The contribution to the change in vibrational state comes as e^{iks_1} in Eq. (4). Since κ is small, a Taylor expansion gives

$$\begin{aligned} e^{iks_1} &= 1 + iks_1 - \frac{k^2 s_1^2}{2} + \cdots \\ &= 1 + i\kappa(a_1^\dagger + a_1) - \frac{\kappa^2}{2}(a_1^\dagger + a_1)^2 + \cdots . \end{aligned} \tag{19}$$

Since the laser interacts with the density matrix through the coherence terms, the orders of the transitions to the population from the first-order and second-order terms are κ^2 and κ^4, respectively. Hence, the energy deposited is primarily contributed by the first-order term.

When there is a continuous laser incident on the atoms, the electronic internal states of the atoms reach a steady state. Instead of the total recoil energy and momentum deposited, we calculate the rate of recoil deposited in the atoms by time evolving the density matrix using Eq. (2). Figure 1 shows the energy deposited per incident photon in the direction of the incident laser on a single atom as we vary the trap frequency. It also shows the contribution of the kick due to the coherent laser interaction and the decoherent single-atom decay term. To ignore long-term effects like shifts in position due to radiation pressure, the expectation values are taken immediately after reaching electronic steady state. It is important to note that we are discussing the transfer of energy across different trap frequencies and not the population in the excited states. As the frequency goes up, the energy difference between the vibrational states will increase. If the energy transfer remains the same but the frequency goes up, there will necessarily be a lower population in excited vibrational states.

The atom absorbs a photon and randomly emits it in an arbitrary direction. At low trap frequencies, the absorption of the photon results in E_r recoil, and the emission gives $0.4E_r$ in the laser direction. The recoil due to the emission agrees with the result in Eq. (18) and is independent of the trap frequency. But as we increase the frequency, the contribution for vibrational excitation from the laser becomes negligible. At low trap frequencies ($\omega_t \ll \Gamma$), the vibrational energy states are close enough that the linewidth spread of the excited state can allow vibrational transitions. On the other hand, at high trap frequencies ($\omega_t \gg \Gamma$), the vibrational energy states are far enough apart that there are no vibrational transitions due to the laser. Hence, the kick from the laser reduces when the trap frequency is higher than the decay rate of the system. Effects such as sideband cooling can also be seen when the trap frequencies are higher than the decay rate.

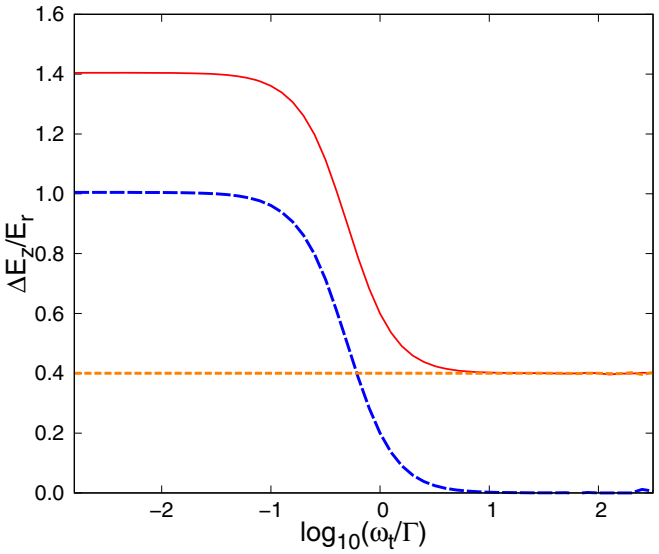

FIG. 1. The vibrational energy deposited, per incoming photon, at steady state for a laser incident on a single atom. The red solid line shows the total energy deposited, while the blue long-dashed and orange short-dashed lines show the contributions from the coherent laser transfer and the decoherent decay. The calculations were run using $N_{\text{vib}} = 5$.

2. Coherent and decoherent transfers

There are two types of vibrational population transfers occurring in the system. When the *population* transfers through the coherence terms (off-diagonal terms) of the density matrix, it is called coherent transfer. This is a two-step process in which the initial population terms couple to coherence terms which then couple to population terms in different vibrational states, ultimately leading to a change in vibrational energy. Hence, any coherent transfers of the order of κ^2 will lead to a population change of the order of κ^4. The transfers due to the laser Hamiltonian are an example.

Decoherent transfers occur when the population directly transfers between the diagonal terms, without going through the coherence terms. This can be seen in the second line of Eq. (17), where there is a direct single-level transition from the $|0\rangle\langle 0|$ to $|1\rangle\langle 1|$ vibrational state. Since the trap Hamiltonian acts on only the coherence terms, it does not affect the dynamics of the decoherent transfers. Hence, the decoherent *energy* transfers, such as the single-atom decay term, are unaffected by the trap frequency.

B. Multiatom decay

When there is more than one atom interacting, the H_{dd} Hamiltonian [Eq. (6)] and the two atom Lindblad terms [i.e., $i \neq j$ terms in Eq. (7)] come into effect. Since the vibrational raising and lowering operators in these terms act on different atoms, they cannot directly transfer the vibrational population.

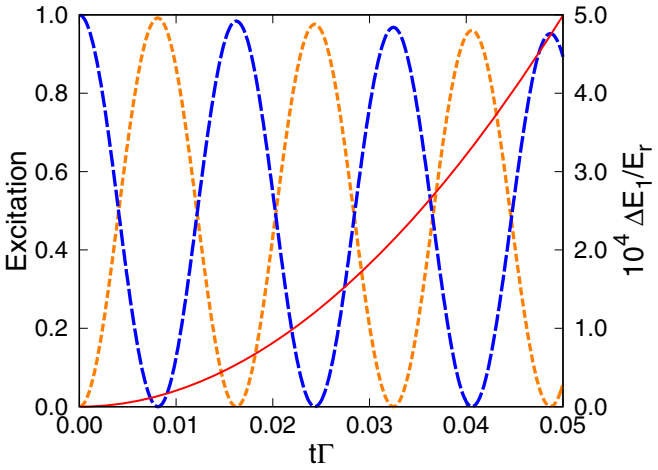

FIG. 2. The excitation is exchanged between two atoms which are very close to each other ($d = 0.02\lambda$) when one atom is initially excited. The orange short-dashed and blue long-dashed lines indicate the excitation probability of the two atoms. The red solid line shows the increase in the vibrational energy of the first atom. The calculation was done using $\kappa = 0.00001$ and $N_{\text{vib}} = 2$ using the full density matrix.

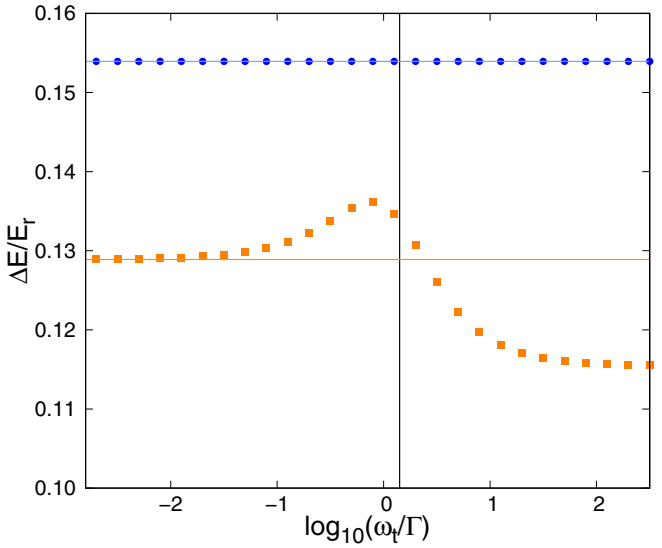

FIG. 3. The energy deposited during the decay of two atoms uniformly excited, separated by $d = 0.4\lambda$ in the x direction, versus the trap frequency. The blue circles and orange squares indicate the quantum harmonic-oscillator model results in the z and x directions, respectively. The thin solid lines indicate the respective impulse model result. The black vertical line denotes the collective decay rate of the system. The calculations are done using the full density matrix with $\kappa = 0.001$. To isolate the effects of the trap frequency, κ is kept constant, and the mass M is varied to compensate for changing ω_t.

They go through the coherence terms and are coherent population transfers (see Sec. III A 2).

For simplicity, we can look at the case of two atoms. When two atoms are very close to each other ($d \approx 0.02\lambda$) and one of the atoms is excited, the excitation rapidly hops between the two atoms while decaying, as seen from Fig. 2. This is the resonant dipole-dipole interaction arising from the Hamiltonian term in Eq. (6). Even though the excitation probability of the atom alternates, the recoil energy deposited on the atom increases continuously. All the recoil in this timescale comes from the near-field dipole-dipole interactions, i.e., from the two-atom dipole-dipole Hamiltonian [Eq. (6)].

When two atoms interact, the direction along the line connecting the atoms and the directions perpendicular have considerably different physics. Let the atoms be separated in the x direction by a distance $d < \lambda$. In the direction along the separation, i.e., in the x direction, interatom forces arise due to the collective interactions. These forces act only along the line joining the two atoms. In the directions perpendicular to the separation, i.e., the y and z directions, there are no interatom forces, and only the kick from the photon emitted contributes to the recoil.

In Figs. 3 and 4, κ is held constant while the trap frequency is altered. Since κ depends on M and ω_t, we assume that the mass also varies accordingly to compensate. While this is not a physical assumption, it is made in order to study and isolate the effects of the change in trap frequency while ignoring the more trivial effects of altering the spread of the wave function.

1. Transverse oscillation

For two atoms, when the chosen direction of vibrational quantization is perpendicular to the separation of the atoms, there are no interatom forces. While taking the Taylor expansion, the first derivative of the Green's function $g'(\mathbf{R}_{ij})$ in the direction perpendicular to the separation is zero. This results in the equations being similar to the equations for the single-atom case, where only zero- and second-order terms remain. But since the two-atom Lindblad terms are coherent transfers, the second-order term of κ^2 will contribute to only a κ^4 order of vibrational population transfer. Hence, we see that in the perpendicular direction, only the contribution from the single-atom Lindblad terms contribute to the change in vibrational energy to the lowest order in κ. The single-atom terms being decoherent transfers also implies that the energy deposited in the perpendicular direction is independent of the trap frequency. Thus, the impulse model is valid even beyond the sudden approximation in the directions where there are no interatom interactions i.e., perpendicular to the atom array.

Figure 3 shows that the recoil in the perpendicular direction is independent of the frequency and agrees with the impulse model calculations. In Figs. 3 and 4, the atoms are initially excited to a singly excited state with the amplitude of the electronic excitation distributed uniformly or to an eigenstate of the complex Green's-function matrix of the system. There is no laser interaction, and the recoil is measured after the system is allowed to decay into the electronic ground state. Further details are included in Sec. III A of Ref. [25].

Another inference is that the rate of energy deposited into the system is dependent on only the single-atom terms and is not directly dependent on the collective decay dynamics. The single-atom term results in the rate of increase of the electronic ground state and, indirectly, the rate of accumulation of vibrational excitation being proportional to the excitation in the system. However, the collective decay dynamics is what determines the lifetime of the excitation. If we integrate the vibrational excitation accumulation over the entire decay

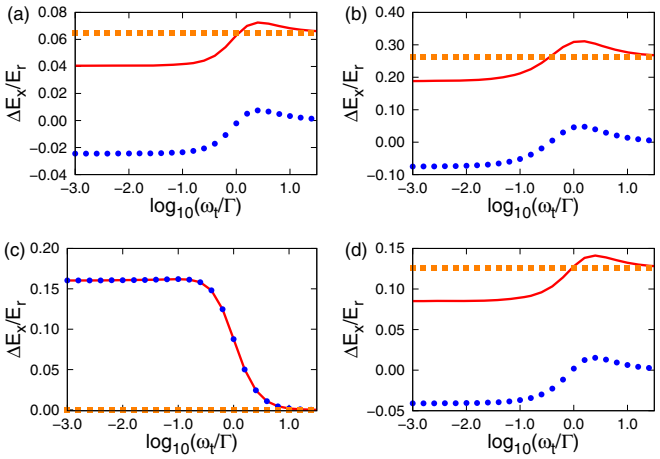

FIG. 4. The vibrational energy deposited during the decay of the excitation. We look at the energy deposited in the x direction on the center atom when there are three atoms in a line in the x direction separated by $d = 0.4\lambda$. The red solid line shows the total energy deposited, while the blue circles and orange squares show the contributions from the coherent and decoherent transfers, respectively. The initial excitation is different for the four cases. (a) has uniform excitation, and (b)–(d) have the three eigenstates as excitation. The increase or decrease in energy is dependent on the excitation pattern in the higher-ω_t region. (c) has zero decoherent transfers because the center atom has zero excitation probability in this particular eigenstate. The calculations are done using the full density matrix with $\kappa = 0.001$. To isolate the effects of the trap frequency, κ is kept constant, and the mass M is varied to compensate for changing ω_t.

process, the energy deposited in such a collective decay will be proportional to the lifetime of the collective excitation. This was also discussed in Sec. III A of Ref. [25].

2. Longitudinal oscillation

In the case of the oscillations in the direction of the separation, the first derivative $g'(\mathbf{R}_{ij})$ in Eq. (9) is no longer nonzero. These first-order coherent transfers contribute to a κ^2 order of population transfer. Hence, there are two sources of vibrational excitation: single-atom decoherent transfers and first-order two-atom Lindblad coherent transfers. While the former is unaffected by the trap Hamiltonian, the latter interacts and develops a complicated dependence on the trap Hamiltonian. Figure 3 shows that the recoil in the direction of separation is dependent on the trap frequency and the impulse model is not valid beyond the sudden approximation.

Figure 4 shows an example of the energy deposited in the direction of separation varying with ω_t when the atoms are initially excited in different distributions. The contributions from the coherent and decoherent transfers are also shown. The decoherent transfers are independent of the trap frequency and depend on only the excitation probability of that atom and the decay rate of the system. The coherent transfers, on the other hand, change with the trap frequency and are highly dependent on the way the excitation is distributed among the atoms and can be either negative or positive. The threshold of what determines high trap frequency is set by the collective decay rate of the system and not the individual decay rate of the atom Γ.

Another distinguishing feature of the coherent and decoherent transfers is the directionality. The coherent transfers are facilitated by the near-field dipole-dipole interaction between the two atoms, and the recoil in this process is strictly in the direction of separation. The laser interaction is also coherent and has a strict directionality with respect to the direction of the incident light. On the other hand, the decoherent transfer is from spontaneous decay, where the direction of photon emission is random and the probability distribution of the direction is governed by the dipole orientation.

C. Large ensemble of atoms

From Sec. II, the number of states required for calculations increases exponentially with increasing the number of atoms. All the atoms having N_{vib} vibrational states would result in all the possible permutations of vibrational-state ensembles, i.e., $(N_{\text{vib}})^N$ states.

While the internal-state dynamics of absorption, decay, and exchange in excitation are the driving factors of the dynamics of the vibrational states, in the approximation in which the spread of the wave function is much smaller than the distance separating the atoms, we see that the vibrational-state dynamics have little to no effect on the internal-state dynamics. Hence, we can approximate the calculation so that only one atom is allowed to have quantized vibrational states while the rest are fixed in space. This reduces the total available vibrational states to just N_{vib}. We calculated the vibrational energy acquired when four atoms in a square are initially excited and decay into the ground state. The error when using this approximation is only 0.2% when the wave-function spread is as high as 25% of the separation.

We also see from Sec. III B that the second-order transfers in the vibrational state are of the order of κ^4. When taking the expectation of the energy, they hardly contribute when κ is small. The same reasoning applies to the lasers (as seen in Sec. III A). Hence, we can limit N_{vib} to 2 without losing generality in this case. For small enough $\kappa = 0.01$, the maximum vibrational energy in the atom can reach up to $10^4 E_r$, which is within the expected recoil limits. To verify this, the results were tested for convergence using different N_{vib} in a small number of atoms.

With these two approximations, we can limit the number of states to $N_{\text{vib}} \times (N + 1)$, that is, $2(N + 1)$, which brings it within the realm of computation for up to 250 atoms.

1. Arrays of atoms

If there is a constant laser incident perpendicular to an array of closely packed atoms, the recoils in the two different directions have different behaviors. Since the laser Hamiltonian does not have two-atom interactions, the recoil of the atoms in the direction perpendicular to the array is similar to the single-atom laser interaction seen in Sec. III A 1. The recoil within the plane of the array is due to the in-plane collective decay effects, as seen in Sec. III B, and is dependent on the distribution of the excitation. Figure 5 shows the trend of the recoil in the different directions as a function of the trap

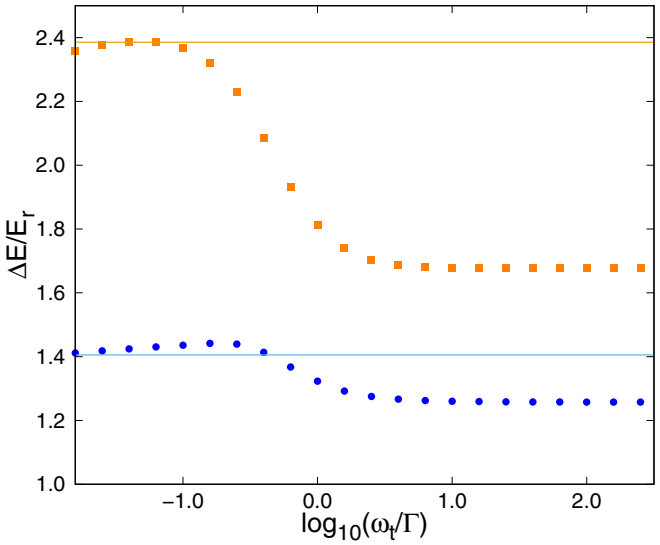

FIG. 5. The vibrational energy deposited in the center atom of an 11×11 atom array with $d = 0.8\lambda$ separation when in steady state with an incident laser in the z direction. The orange squares represent the recoil energy in the z direction, while the blue circles denote the recoil energy in the x direction, per photon incident on the center atom. The upper orange and lower blue thin lines denote the comparison with the impulse model. These data are calculated using the approximations discussed in Sec. III C.

frequency. The calculations from the impulse model are also included as a solid line.

Typically, the trap frequencies in the in-plane (x and y) directions are higher and are about 100 kHz, while the perpendicular trap frequencies are often an order of magnitude lower at about 10 kHz. These trap frequencies will give a spread of $\kappa/k = 0.08\lambda$ and 0.025λ, respectively, for a Cs atom. When in a steady state, such frequency ranges will be within the slow-oscillation approximation, and the results from the impulse model can be reproduced with the current model.

When there is a perfect reflection of a photon from an atom array, there is a momentum of $2\hbar k$ imparted on the atoms. Hence, the momentum change of the atoms describes the reflectivity of the atom array. This can also be used to study the effects of higher vibrational excited states on the reflectivity. At 10-kHz frequency in the z direction, the momentum imparted on the central atom of an array reduces by approximately 8% when the atom is in the first vibrational excited state instead of in the ground state. However, at 100-kHz frequency in the z direction, there is only a decrease of 0.6%. This reinforces that atomic mirror experiments would need to have high trap frequencies to have a reflection probability close to 1.

2. Cavity

In Ref. [25], we calculated the kinetic-energy kick on a cavity when it decays from a highly subradiant eigenmode. This follows the design of the cavity used in Ref. [13] to perform quantum information processing. Under the slow-oscillation approximation, the central atom experienced a kick of up to $926E_r$ in the duration of the decay in the direction perpendicular to the plane. The results were thought to be purely qualitative because of the large lifetimes violating the slow-oscillation approximation.

The results from the Sec. III B imply that those calculations were more accurate than suggested in Ref. [25] for the direction perpendicular to the array. In the perpendicular direction, since there are no or negligible interatom forces, the trap frequency does not play a significant role in determining the vibrational energy deposited. The recoil due to the decoherent transfers accumulates over an extended duration due to the subradiant decay resulting in large recoil energies being deposited. Another way to interpret this is the large quality factor causing there to be multiple reflections of the photon on the array faces.

Calculations for the same cavity as that in Ref. [25], using the harmonic-oscillator model, resulted in the center atom experiencing similar vibrational energy being deposited, approximately $922E_r$ in the direction perpendicular to the array. This recoil was unaffected when the trap frequencies were increased beyond the decay rate of the system. On the other hand, the energy deposited in the in-plane direction at high frequencies decreased to $15.0E_r$, compared to $16.6E_r$ at low frequencies. These results show that the recoil of the atoms due to collective decay, especially in highly subradiant systems, should not be ignored.

IV. CONCLUSION

We presented a model to describe and calculate the recoil in light-matter collective interaction using quantum harmonic-oscillator trap potentials. We compared our results with the results of the impulse model used in Ref. [25] under the slow-oscillation approximation and explored the regime beyond. We studied the contribution to recoil from the different terms of the Hamiltonian and Lindblad equation. In essence, the single-atom Lindblad term causes a recoil in a random direction, and the energy deposited is independent of the trap frequency used. The laser Hamiltonian causes a recoil in the direction of the laser propagation, and recoil energy deposited falls off to zero when the trap frequency goes beyond the collective decay rate of the system. The two-atom Lindblad terms induce a recoil in the direction of the separation between the atoms, and it is dependent on both the trap frequency and the distribution of the excitation in the system.

In atom arrays, in the directions where there are no interatom forces or lasers, the recoil is independent of trap frequency, and the impulse model can be used even beyond the slow-oscillation approximation. If the atoms are excited by a laser or for those directions in the plane of the atom array, the impulse model is no longer valid when the trap frequency approaches or is higher than the decay rate of the system.

This model was used to verify the extremely high recoil calculated in a cavity with high subradiance. This shows that recoil effects have to be considered seriously when working with highly subradiant systems. The effects of vibrational excitation in the reflectivity of arrays were also studied.

References [26,27] worked on the opposite regime of the sudden approximation, where the focus is on the slow center-of-mass motion rather than the fast internal-state dynamics.

Studying this regime, especially the collective modes of vibration of the atoms using the quantum harmonic-oscillator model, could lead to better understanding and control of atom arrays.

Data for the figures used in this publication are available from the Purdue University Research Repository [28].

ACKNOWLEDGMENTS

This work was supported by the National Science Foundation under Award No. 2109987-PHY. This research was supported in part through computational resources provided by Information Technology at Purdue University, West Lafayette, Indiana.

[1] R. H. Dicke, Coherence in spontaneous radiation processes, Phys. Rev. **93**, 99 (1954).
[2] R. J. Bettles, S. A. Gardiner, and C. S. Adams, Cooperative ordering in lattices of interacting two-level dipoles, Phys. Rev. A **92**, 063822 (2015).
[3] N. E. Rehler and J. H. Eberly, Superradiance, Phys. Rev. A **3**, 1735 (1971).
[4] R. Friedberg, S. R. Hartmann, and J. T. Manassah, Frequency shifts in emission and absorption by resonant systems of two-level atoms, Phys. Rep. **7**, 101 (1973).
[5] M. Gross, C. Fabre, P. Pillet, and S. Haroche, Observation of Near-Infrared Dicke Superradiance on Cascading Transitions in Atomic Sodium, Phys. Rev. Lett. **36**, 1035 (1976).
[6] M. O. Scully, Collective Lamb Shift in Single Photon Dicke Superradiance, Phys. Rev. Lett. **102**, 143601 (2009).
[7] Z. Meir, O. Schwartz, E. Shahmoon, D. Oron, and R. Ozeri, Cooperative Lamb Shift in a Mesoscopic Atomic Array, Phys. Rev. Lett. **113**, 193002 (2014).
[8] J. Pellegrino, R. Bourgain, S. Jennewein, Y. R. P. Sortais, A. Browaeys, S. D. Jenkins, and J. Ruostekoski, Observation of Suppression of Light Scattering Induced by Dipole-Dipole Interactions in a Cold-Atom Ensemble, Phys. Rev. Lett. **113**, 133602 (2014).
[9] A. Browaeys, D. Barredo, and T. Lahaye, Experimental investigations of dipole–dipole interactions between a few Rydberg atoms, J. Phys. B **49**, 152001 (2016).
[10] S. L. Bromley, B. Zhu, M. Bishof, X. Zhang, T. Bothwell, J. Schachenmayer, T. L. Nicholson, R. Kaiser, S. F. Yelin, M. D. Lukin, A. M. Rey, and J. Ye, Collective atomic scattering and motional effects in a dense coherent medium, Nat. Commun. **7**, 11039 (2016).
[11] D. Plankensteiner, C. Sommer, H. Ritsch, and C. Genes, Cavity Antiresonance Spectroscopy of Dipole Coupled Subradiant Arrays, Phys. Rev. Lett. **119**, 093601 (2017).
[12] S. Jennewein, L. Brossard, Y. R. P. Sortais, A. Browaeys, P. Cheinet, J. Robert, and P. Pillet, Coherent scattering of near-resonant light by a dense, microscopic cloud of cold two-level atoms: Experiment versus theory, Phys. Rev. A **97**, 053816 (2018).
[13] P.-O. Guimond, A. Grankin, D. V. Vasilyev, B. Vermersch, and P. Zoller, Subradiant Bell States in Distant Atomic Arrays, Phys. Rev. Lett. **122**, 093601 (2019).
[14] J. P. Clemens, L. Horvath, B. C. Sanders, and H. J. Carmichael, Collective spontaneous emission from a line of atoms, Phys. Rev. A **68**, 023809 (2003).
[15] B. Yan, S. A. Moses, B. Gadway, J. P. Covey, K. R. A. Hazzard, A. M. Rey, D. S. Jin, and J. Ye, Observation of dipolar spin-exchange interactions with lattice-confined polar molecules, Nature (London) **501**, 521 (2013).
[16] V. Mkhitaryan, L. Meng, A. Marini, and F. J. G. de Abajo, Lasing and Amplification from Two-Dimensional Atom Arrays, Phys. Rev. Lett. **121**, 163602 (2018).
[17] S. D. Jenkins, J. Ruostekoski, N. Papasimakis, S. Savo, and N. I. Zheludev, Many-Body Subradiant Excitations in Metamaterial Arrays: Experiment and Theory, Phys. Rev. Lett. **119**, 053901 (2017).
[18] R. Bekenstein, I. Pikovski, H. Pichler, E. Shahmoon, S. F. Yelin, and M. D. Lukin, Quantum metasurfaces with atom arrays, Nat. Phys. **16**, 676 (2020).
[19] A. Grankin, P. O. Guimond, D. V. Vasilyev, B. Vermersch, and P. Zoller, Free-space photonic quantum link and chiral quantum optics, Phys. Rev. A **98**, 043825 (2018).
[20] Y. Wang, X. Zhang, T. A. Corcovilos, A. Kumar, and D. S. Weiss, Coherent Addressing of Individual Neutral Atoms in a 3D Optical Lattice, Phys. Rev. Lett. **115**, 043003 (2015).
[21] R. J. Bettles, S. A. Gardiner, and C. S. Adams, Enhanced Optical Cross Section via Collective Coupling of Atomic Dipoles in a 2D Array, Phys. Rev. Lett. **116**, 103602 (2016).
[22] E. Shahmoon, D. S. Wild, M. D. Lukin, and S. F. Yelin, Cooperative Resonances in Light Scattering from Two-Dimensional Atomic Arrays, Phys. Rev. Lett. **118**, 113601 (2017).
[23] J. Rui, D. Wei, A. Rubio-Abadal, S. Hollerith, J. Zeiher, D. M. Stamper-Kurn, C. Gross, and I. Bloch, A subradiant optical mirror formed by a single structured atomic layer, Nature (London) **583**, 369 (2020).
[24] F. Robicheaux and S. Huang, Atom recoil during coherent light scattering from many atoms, Phys. Rev. A **99**, 013410 (2019).
[25] D. A. Suresh and F. Robicheaux, Photon-induced atom recoil in collectively interacting planar arrays, Phys. Rev. A **103**, 043722 (2021).
[26] E. Shahmoon, M. D. Lukin, and S. F. Yelin, Quantum optomechanics of a two-dimensional atomic array, Phys. Rev. A **101**, 063833 (2020).
[27] E. Shahmoon, M. D. Lukin, and S. F. Yelin, Collective motion of an atom array under laser illumination, in *Advances In Atomic, Molecular, and Optical Physics* (Academic Press, Cambridge, MA, 2019), Vol. 68, pp. 1–38
[28] D. A. Suresh and F. Robicheaux, Data for: Atom recoil in collectively interacting dipoles using quantized vibrational states, Purdue University Research Repository, https://doi.org/10.4231/BPXW-D303.